Sub-10 nm Nanofabrication *via* Nanoimprint Directed Self-Assembly of Block Copolymers

Sang-Min Park,[†] Xiaogan Liang,[†] Bruce D. Harteneck,[†] Teresa E. Pick,[†] Nobuya Hiroshiba,[†] Ying Wu,[†,‡] Brett A. Helms,[†,*] and Deirdre L. Olynick[†,*]

[†]The Molecular Foundry, Lawrence Berkeley National Laboratory, One Cyclotron Road, Berkeley, California 94720, United States and,[‡]Oxford Instruments America, Inc., 300 Baker Avenue, Suite 150, Concord, Massachusetts 01742, United States

ABSTRACT Directed self-assembly (DSA) of block copolymers (BCPs), either by selective wetting of surface chemical prepatterns or by graphoepitaxial alignment with surface topography, has ushered in a new era for high-resolution nanopatterning. These pioneering approaches, while effective, require expensive and time-consuming lithographic patterning of each substrate to direct the assembly. To overcome this shortcoming, nanoimprint molds—attainable *via* low-cost optical lithography—were investigated for their potential to be reusable and efficiently template the assembly of block copolymers (BCPs) while under complete confinement. Nanoimprint directed self-assembly conveniently avoids repetitive and expensive chemical or topographical prepatterning of substrates. To demonstrate this technique for high-resolution nanofabrication, we aligned sub-10 nm resolution nanopatterns using a cylinder-forming, organic–inorganic hybrid block copolymer, polystyrene-*block*-polydimethylsiloxane (PS-*b*-PDMS). Nanopatterns derived from oxidized PDMS microdomains were successfully transferred into the underlying substrate using plasma etching. In the development phase of this procedure, we investigated the role of mold treatments and pattern geometries as DSA of BCPs are driven by interfacial chemistry and physics. In the optimized route, silicon molds treated with PDMS surface brushes promoted rapid BCP alignment and reliable mold release while appropriate mold geometries provided a single layer of cylinders and negligible residual layers as required for pattern transfer. Molds thus produced were reusable to the same efficacy between nanoimprints. We also demonstrated that shear flow during the nanoimprint process enhanced the alignment of the BCP near open edges, which may be engineered in future schemes to control the BCP microdomain alignment kinetics during DSA.

KEYWORDS: block copolymer self-assembly · directed self-assembly · nanoimprint lithography · nanolithography · nanofabrication

Block copolymer (BCP) lithography is a versatile technique whereby ordered, periodic polymer microdomains (*e.g.*, posts, lines), potentially in controlled geometries (*e.g.*, bends or junctions), are lithographically transferred into substrates.[1−5] There is a significant effort in both academia and industry to apply the technique toward constructing ultrahigh density integrated circuits,[6−9] bit patterned media,[10−13] and other micro- or nanoelectronic architectures.[6,11,12,14] Many of these applications require perfectly aligned, addressable features derived from selective removal of one of the BCP microdomains and etching through the underlying substrate. In these cases, conventional (untemplated) BCP self-assembly, with its inherent defect propensity, is generally insufficient for precision, large-area nanofabrication. Directed self-assembly (DSA) of BCP thin films has been used to impose a greater level of control and order over the assembly process, toward defect-free BCP-derived nanoscale features. Two general approaches for DSA have emerged: (1) graphoexpitaxy with topographic patterns on the substrate to guide BCP microphase separation and ordering;[11,15−17] and (2) surface chemical patterning, where patterned regions of hydrophobic and hydrophilic character at the substrate preferentially attract one block over the other due to differences in interfacial free energy.[4,8,18] Both techniques have produced impressive density multiplication and pattern defect self-correction with resolutions that are difficult or impossible to achieve with top-down techniques alone. The major drawback of these approaches is that every substrate must be prepatterned to direct the BCP ordering, which requires costly lithographic steps.[4,15] Furthermore, another drawback in graphoepitaxial driven alignment is that the topographic pattern created to drive the alignment must be incorporated or eliminated—with additional processing steps—from the final nanofabricated structure. Methodologies detailing alignment in removable silicon[6] or disposable, lithographically defined polymer templates have emerged,[19−22] whereas others have incorporated the template within the BCP domains.[5] However, in the latter case, line edge roughness is a potential problem. Here, we present a robust procedure, using thermal nanoimprint lithography, for DSA of BCPs which avoids any type of substrate prepatterning and is particularly suited to

* Address correspondence to dlolynick@lbl.gov, bahelms@lbl.gov.

Received for review April 15, 2011 and accepted October 13, 2011.

Published online October 13, 2011
10.1021/nn201391d

the types of highly planar surfaces found in integrated circuit and magnetic media production.

DSA of BCPs *via* nanoimprint has been a largely underexplored area in nanofabrication in part due to mold release issues. Mold release in nanoimprint technology persists as a significant obstacle to achieving reliable, high-quality patterning at the nanoscale. Owing to the inherent high surface area contact between the mold and the imprinted film, the interfacial adhesion is often too high for efficient release, leaving behind damaged, deformed, or delaminated features and sullying the mold.[23] There are several approaches to achieving reliable release in nanoimprint[24] such as fluoroalkyl passivation of hard molds[25] or preparing elastomeric molds from cross-linked perfluoropolyethers;[26] however, direct imprint of BCPs with microphase-segregated morphologies is nevertheless exceptionally challenging without the use of additives.[27] Compounding the problem of DSA of BCPs under nanoimprint is that release requires both preferentially attracting one of the blocks to the template while concomitantly requiring the BCP film to order *via* graphoepitaxy and then release cleanly. An early report from Huck and Li highlights these challenges: BCP ordering in their imprint format was limited to ~2−3 rows of upstanding cylinders, with the domains suffering from poor size uniformity due to the mold's line edge roughness and poor control of the film thickness.[28] Recent work by Man *et al.* showed similar results.[29] Kim *et al.* further identified that, in deep templates, the ordering of the BCP microdomains was frustrated by confinement induced by both the substrate and the template.[30]

Toward a universal procedure for BCP NIL, which has the benefit of avoiding tedious substrate prepatterning, we have developed and report here a thermal imprint strategy for graphoepitaxy-based alignment of BCP microdomains (Figure 1a). We employ the strongly segregating BCP polystyrene-*block*-polydimethylsiloxane (PS-*b*-PDMS) whose relatively high Flory−Huggins parameter ($\chi = 68/T - 0.037$) allows microdomains to form which are smaller than in BCPs with lower Flory−Huggins parameters (same chain lengths and relative volume fractions).[31] Results are presented for PS-*b*-PDMS with 20 nm domain period (L_0), which we and others have shown to be a candidate for sub-10 nm lithography.[27,32−34]

To overcome the challenge of mold release during nanoimprint for DSA of BCP, our group[27] previously used interface segregating surfactants which reduced mold−BCP interfacial adhesion following thermal nanoimprint. While interface segregating surfactants provide excellent release and facilitate alignment of the BCP microdomains, the mold was not reusable without reapplying a fluoroalkylsilane (FAS) surface treatment between imprints. This limits the potential for high-throughput processing of multiple imprinted

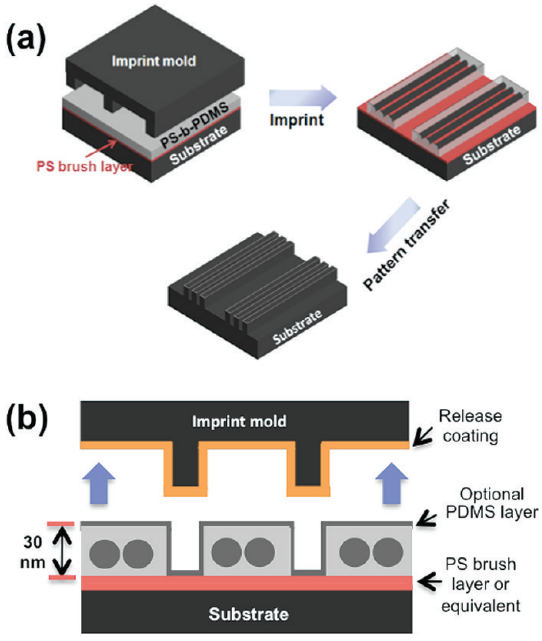

Figure 1. Schematic showing general process and geometric and interface considerations for direct imprinting of cylinder-forming PS-*b*-PDMS for BCP domain alignment. (a) Thermal nanoimprint induces the alignment of cylindrical domains along the length direction of mold patterns. No substrate prepatterning is necessary, and molds are reusable without further chemical manipulation. The aligned PDMS cylinders were used as a template for pattern transfer of sub-10 nm patterns onto the underlying substrates. (b) BCP wetting conditions and equilibrium thickness is determined by the mold and substrate interfaces. The substrate was coated with a layer that attracts the majority PS block. The mold was treated to promote release and alignment. When PDMS is attracted to the mold treatment, the equilibrium thickness for 1 layer of cylinders is 30 nm (1.5 L_0, the natural period of the BCP). When the PDMS layer is absent (majority block attracted to mold), the equilibrium thickness is 20 nm (1 L_0).

films. Aiming to further advance the technique for high-throughput processing and pattern transfer, we investigate poly(dimethyl siloxane) (PDMS), polystyrene (PS), and FAS mold treatments toward reusable molds that do not require interface segregating surfactants. We find that BCP NIL with PS-*b*-PDMS is decidedly unusual in that fluoroalkylsilanes are not suitable interfacial release agents when using silicon hard molds; chemisorbed PDMS brush in place of more widely used fluoroalkylsilanes acts as a robust release agent for the releasing of PS-*b*-PDMS BCP. We show that this result cannot be explained by simple arguments regarding the work of adhesion required. Beyond release agents, in this paper, we demonstrate that the mold design is responsible for flow-enhanced alignment and elimination of the residual layer, which is needed for sub-10 nm plasma pattern transfer. With imprint driven DSA, alignment was achieved in as little as 1 h from applied pressure to release, significantly shorter than that reported for graphoepitaxy techniques in this BCP system using solvent and vacuum annealing[32−34] or with nanoimprint in other systems.[28−30] Finally,

using a new combination of processes and an appropriate BCP/substrate interlayer, a single layer of 8 nm PDMS cylindrical domains was used as a mask to plasma etch well-defined 8 nm lines in a planar silicon dioxide substrate at a 20 nm pitch without the need for an additional hard mask. Hence with nanoimprint-based DSA of BCP, we have achieved a high-throughput, highresolution, process for DSA which eliminates substrate prepatterning or hard mask fabrication for pattern transfer.

RESULTS AND DISCUSSION

Considerations for BCP Lithography and Pattern Transfer Using Nanoimprint DSA. The general process steps for nanoimprint DSA of PS-*b*-PDMS BCP are shown in Figure 1a, while the interface and geometric considerations are shown in Figure 1b. Steps were designed for high-fidelity pattern transfer compatibility. First, a layer is deposited on the substrate that attracts the majority block of the block copolymer. This prevents a PDMS layer forming at the substrate interface, which ultimately decreases etching selectivity to the underlying substrate. Both a PS brush and a Transpin layer (Molecular Imprints, Inc.) attract the majority PS domain, whereas bare silicon or silicon dioxide would attract a PDMS layer. After BCP microdomain alignment *via* thermal imprint and release, the material above and between the PDMS cylinders is etched down to the substrate. The remaining oxidized PDMS and patterned polymeric material just below act as a mask for subsequent pattern transfer to the underlying substrate. By including a polymer such as Transpin in the stack, which is spun thicker than the PS polymer brush, etching selectivity to the underlying substrate is improved.

For high-fidelity plasma pattern transfer of a well-defined BCP defined, it is important to both release the mold after imprint and minimize the residual layer under the protrusive features of the stamp. Release layers and mold geometry were investigated toward that end. Hard molds were used to maintain pattern fidelity and aid residual layer removal during the high-pressure thermal imprint process because soft molds, such as PDMS, have reduced mechanical and thermal stability.[35]

In addition, for lithographic pattern transfer, a single layer of cylinders must be produced. This is determined by both the mold height and the BCP equilibrium film thickness. The equilibrium thickness is, in turn, determined by the interaction of the mold treatment with the blocks of the PS-*b*-PDMS. Three mold treatments were investigated, FAS and brushes of either PDMS or PS. Both FAS and PDMS attracted the PDMS layer, producing an asymmetric wetting condition with an equilibrium thickness of 30 nm (1.5 L_0, the natural period of the BCP, Figure 1b), whereas a PS mold treatment produces a symmetric wetting condition with an equilibrium thickness of ~1 L_0. Mold heights were varied to produce single and multiple layers of cylinders.

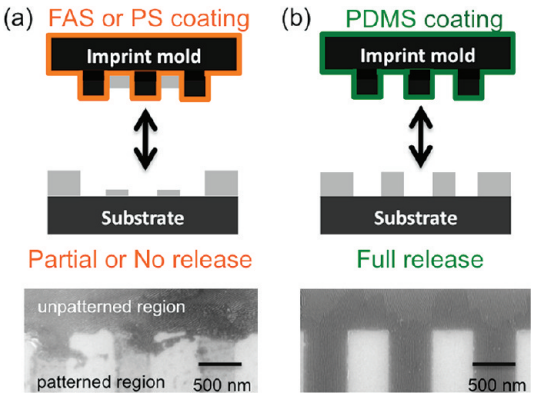

Figure 2. Imprinting PS-*b*-PDMS with nonreleasing and releasing types of mold surface treatments: (a) FAS-treated mold allowed release only in the nonpatterned regions, while a PS-treated mold did not release from the imprinted film; (b) PDMS-treated molds promoted optimal release of the imprinted BCP film.

Mold Treatment for Releasable and Reusable Molds. For nanoimprint DSA of BCP, or any imprint process for that matter, it is crucial to be able to release the mold. Initially, we investigated vapor-deposited fluoroalkyl monolayers well-known for their high anti-adhesion properties and interfacial energy match with PDMS.[27] These results were compared to molds treated with chemisorbed brushes of either PS or PDMS. BCP mold treatments and release results are summarized in Figure 2. Though widely used in other imprint schemes, we observed with repeated trials that molds passivated with FAS (vacuum deposition, 90 °C, 10 min, water contact angle 107°) only provided release from the BCP thin film outside of the patterned features of the mold (Figure 2a). Within the corrugated mold patterns, the BCP adhered to the mold surface, leaving only a patterned residue on the substrate (Figure 2a). In some experiments, it was possible to obtain good release at 25 °C (*i.e.*, well below the glass transition temperature of PS block), but these results were not consistent. Subsequently, we tested molds treated with FAS up to 16 h to increase FAS coverage, but we did not find any improvement in release. Molds passivated with a PS brush produced even poorer results, as adhesion at the interface between the PS-*b*-PDMS block copolymer and mold surface proved insurmountable; nearly the entire thin film adhered to the imprint mold. In sharp contrast, molds treated with a PDMS brush were easily unmolded from thermally imprinted films of PS-*b*-PDMS (Figure 2b). Molds were used up to 10 times without regenerating the brush. Hence, with PDMS as a release layer, robust and reusable molds for DSA of PS-*b*-PDMS were achieved.

In light of the respective surface energies alone, FAS being the lowest, the adhesion results are rather surprising. The lower bound on the work needed to separate

an interface, W, can be estimated from the interfacial energies of the materials:

$$W\ (\mathrm{mJ}) = w_{12} \times A = (\gamma_1 + \gamma_2 - \gamma_{12})A$$

where γ is the interfacial energy between material 1 and 2 with air, γ_{12} and A_{12} are the interfacial energy and area, respectively, between materials 1 and 2, and w_{12} (mJ/m^2) is the work done per unit area when that interface is reversibly separated.[36] For our respective mold−BCP interfaces (FAS−PDMS, PS−PS, or PDMS−PDMS) and substrate−BCP interface (PS−PS in all cases), the interface requiring the least work input is expected to open when the mold and substrate are slowly separated. Values for W are estimated and summarized in Table 1. In column 3, we show the ratio of $W_{mold}/W_{substrate}$. A value of $W_{mold}/W_{substrate}$ less than unity indicates that the BCP should separate at the mold interface as opposed to the substrate interface. In agreement with Table 1 values, the imprint with the PS-treated mold failed due to separation at the substrate ($W_{mold}/W_{substrate} > 1$), whereas the PDMS-treated mold ($W_{mold}/W_{substrate} < 1$) separated well from the imprinted BCP film. FAS-treated molds failed despite the lower work of adhesion. Previous authors using PDMS-treated molds for nanoimprint[37] cite the lower peel-fracture energy of PDMS over perfluoro groups.[38] In addition, Newby *et al.* showed that FAS interfaces were dominated by interfacial slippage, a frictional loss mechanism, such that the energy to separate from a FAS-treated substrate was much higher than that of a PDMS-treated substrate.[39] Hence, despite the lower interfacial energy of FAS with the BCP, PDMS functions as the better mold release treatment potentially due to the higher friction losses of FAS over PDMS.

TABLE 1. Estimated Work of Adhesion, W,[a] for Substrates and Mold Interfaces

interface, interfacial area	W (mJ)	$W_{mold}/W_{substrate}$
PS−PS substrate, A[b]	81.4 × A	N/A
PS−PS mold, 1.1A[b]	81.4 × 1.1A	1.1
PDMS−PDMS mold, 1.1A[b]	39.8 × 1.1A	0.54
PDMS−FAS mold, 1.1A[b]	32.2 × 1.1A	0.43

[a] For PDMS and PS, we used surface energies[45] of 19.9 and 40.7 mJ/m^2, respectively, consistent with our water contact angle measurements at room temperature of 103 and 92°. For fluoroalkylsilane-modified surfaces, we used Morita *et al.*'s[46] value of 14 mJ/m^2 for FAS as our measured water contact angle of 107° (10 min vacuum vapor deposition and room temperature contact angle measurement) coincided with theirs. With a measured PDMS on FAS contact angle of 52°, we estimated γ_{12} (PDMS−FAS interface) as 1.75 mJ/m^2. [b] The area at the BCP−substrate interface is noted as A, whereas the topographic patterning of the mold increases the area at the mold interface to ∼1.1A.

Mold Geometry for Thickness Control, Residual Layer Removal, and Flow-Enhanced Alignment. With successful release afforded by the PDMS mold passivation strategy, we investigated the role of mold geometry on graphoepitaxial alignment of the PS-*b*-PDMS block copolymer. Patterned gratings in the mold were created at a 1 μm pitch with line widths of 40, 50, and 60% of the pitch. All line widths behaved similarly with regard to the subsequent discussion. The patterned features of the mold had a total area of 1.5 × 10^{-3} cm^2 on the order of 1/1000 of the total mold area (∼2 cm^2).

PDMS-passivated molds with the patterned area recessed, as shown in Figure 3a, were investigated as a

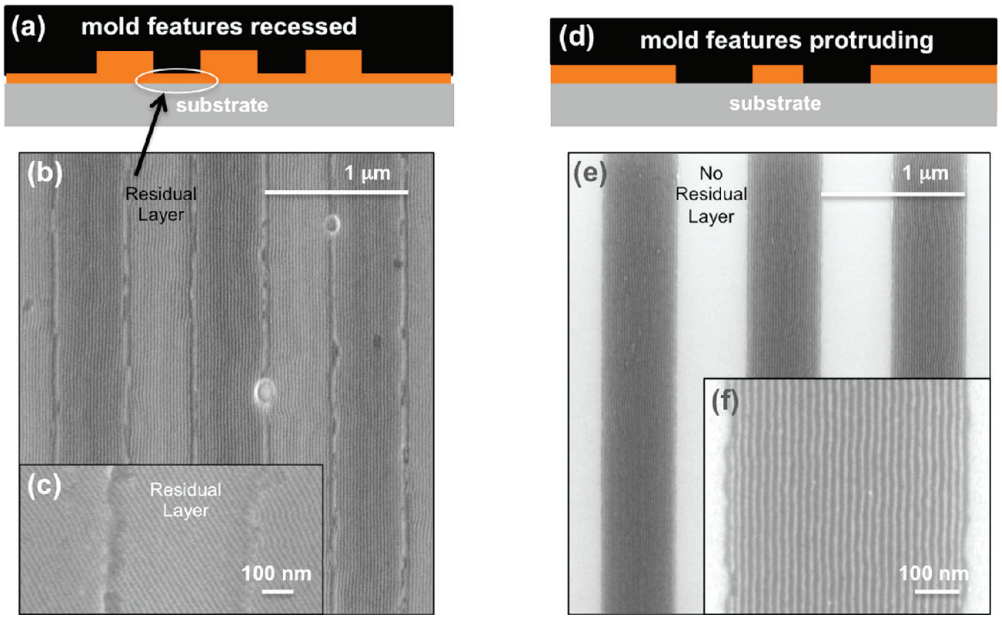

Figure 3. Comparison of two mold geometries: (a) schematic of mold with features recessed; (b) SEM image taken after plasma etch to reveal PDMS cylinders; image shows that a residual layer was present when the molds with recessed features were used; (c) inset shows that PDMS cylinders in the residual layer align with material in molded areas of the BCP film; (d) schematic of mold with features protruding; (e) plasma etching reveals that PDMS cylinders show no evidence of residual layer. (f) Magnified image showing PDMS cylinders aligned along the long axis of the imprint grating.

means to facilitate the thinning and elimination of the block copolymer films outside the patterned region. This is analogous to patterning in negative tone with an optical/UV resist where the patterned features remain, but the film outside the patterned region is removed. BCPs patterned with these molds (Figure 3b) required higher pressures and longer imprint times. This recessed feature mold geometry showed intermittent success in eliminating the residual layer between the features and little ability to thin the film outside the patterned area, even at very high applied imprint pressures (200 psi). In addition, we found that the alignment of cylindrical domains was easily affected by the direction of residual layer domains: undesirable orientation of cylinders was a regular occurrence (Figure 3c). Moreover, with any significant residual layer present, it was difficult to control the molded film thickness, causing the patterned region to contain more than one layer of cylinders.

By comparison, at significantly lower applied pressures (50 psi), the PDMS-passivated molds composed of protrusive features essentially eliminated the residual layer (Figure 3d). After a CF_4 and O_2 etching sequence, no residual layer was present (Figure 3e) and aligned BCP patterns were revealed along the long axis of the grating pattern (Figure 3f). A 20 nm domain period was extracted with fast Fourier analysis. Using myCD software (aBeam Technologies), the cylinder domain widths were measured as 7.7 nm, whereas the 3σ line edge roughness and line width roughness were 2.4 and 2.1 nm, respectively.

With the ability to minimize the residual layer using the molds with protrusive features, we were able to precisely control the imprint thickness with the mold depth, allowing us to tune the number of cylinder layers in the imprinted block copolymer. To achieve a single layer of cylinders under our asymmetric wetting condition, a maximum molded film thickness of 30 nm (*i.e.*, $1.5 \times L_0$) was targeted. Starting with ~24 nm BCP films, we found that 30 nm deep molds produced a single layer of ordered cylindrical domains within the pattern regions without any measurable residual layer (Figure 4a). Imprinting the 24 nm film with deeper molds ~60 nm deep produced layers of stacked, hexagonally packed cylinders aligned parallel to the vertical mold walls (Figure 4b). Given the duty cycle of the imprint mold (~1:1) and the 24 nm film thickness, flow from material reservoir at the end of the grating features is required to fill a 60 nm mold. In addition, we noted that the degree of order was dramatically improved near the open ends of gratings structure. A single layer of cylinders in the 30 nm mold were aligned parallel to the vertical wall of the mold up to ~100 μm from the grating ends, whereas toward the middle of the 500 μm long gratings, the alignment was perpendicular or random. We surmised that flow of the polymer melt[40] was responsible for the

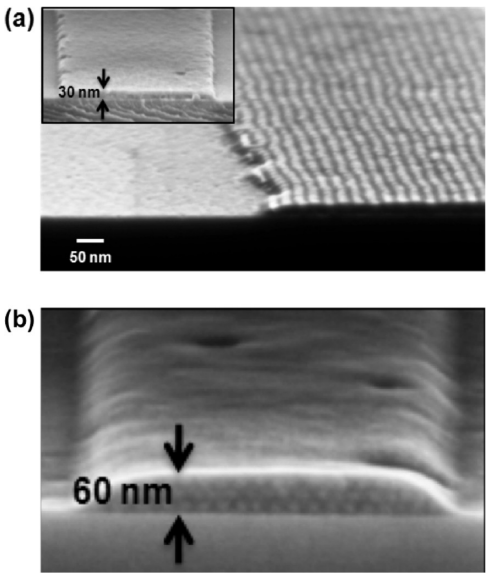

Figure 4. Cross-sectional SEM images of thermal imprinted PS-*b*-PDMS block copolymer patterns using a 30 nm (a) and 60 nm (b) thick mold: (a) 30 nm height as imprinted (inset) and after etching to reveal the cylinders; (b) 60 nm height before etching. Hexagonally packed white spots are stacked cylinders in the cross section.

improved order at the grating edges, where stressed polymer[41] displaced from under the mold protrusions flowed more easily in direction parallel to the grating pattern.

In order to get more insight into the flow behavior of PS-*b*-PDMS during nanoimprint, we designed mold patterns as shown in Figure 5. The closed ring patterned mold predominantly induced cylindrical alignment in the radial direction, as shown in Figure 5a. With this design, polymer displacement during thermal imprinting mainly occurs in a direction normal to the mold sidewalls. On the other hand, for half-ring patterns in Figure 5b, on the other hand, the flow was from the open ends of the ring such that alignment was directed along the sidewall, even for short annealing times. Alignment near the grating edges was noted in annealing times as short as 10 min (10 min at high temperature with 1 h cool before release), significantly shorter than that used to align similar PS-*b*-PDMS using other methods.[27,32−34] In addition, flow promoted alignment of the cylinders outside of the pattern at the length scale of approximately 2 μm. Interestingly, the confluence of two imprint-induced flow directions produced defects (dotted box of Figure 5b). Alignment perpendicular to the sidewalls is not the equilibrium state of the system, and with long annealing times, the preferential interaction between one block and mold surface typically promotes topographic alignment to the sidewall.[8,42] However, longer annealing time under our pressure and temperature conditions caused damage in the BCP. This damage manifested as extremely high line edge roughness at the edges of the domains.

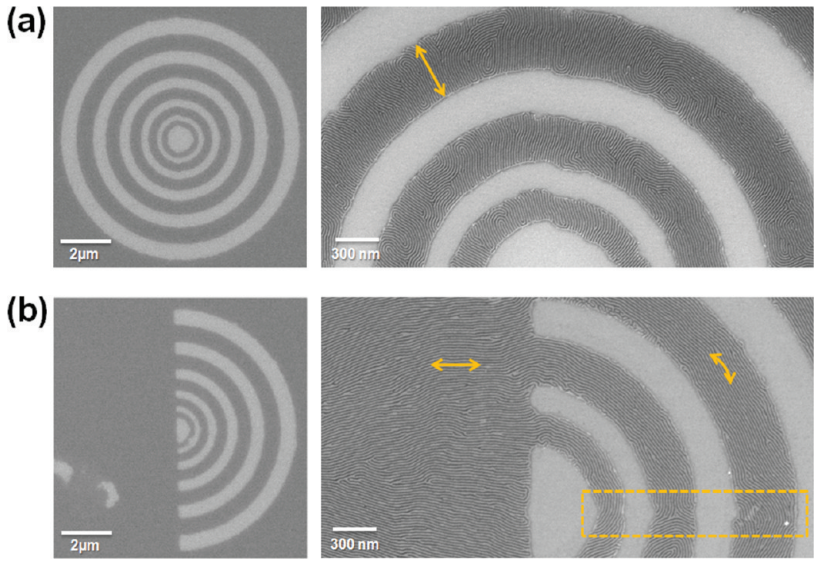

Figure 5. Flow behavior of PS-*b*-PDMS cylindrical domains during thermal imprint in low- (left) and high- (right) magnification SEM images. With a closed-end circular pattern (a), arrow shows that nanoimprint-induced polymer flow promoted cylinder alignment perpendicular to the sidewalls. With an open-ended pattern (b), nanoimprint-induced polymer flow allowed alignment parallel to sidewalls. Rectangle (b) shows that defects arose when flow patterns intersected.

Pattern Transfer of Molded BCP Films into the Underlying Substrate. Using PS-*b*-PDMS films aligned using NIL with PDMS-passivated protrusive molds, we developed a procedure for transferring the highly aligned features into underlying silicon substrates. We found that the process required a sacrificial layer to increase the aspect ratio of transferred patterns. Here we use Transpin as a sacrificial layer, which is a proprietary material available from Molecular Imprints, Inc. Transpin has a water contact angle of 83° (PS contact angle is ~90°), a preferential attraction to PS over PDMS, and strong expected adherence to the PS majoring block during imprint.[43] A 13 nm Transpin layer was first coated onto silicon oxide layer then cross-linked by baking at 180 °C for 10 min. A ~24 nm thin film of PS-*b*-PDMS was then spin-coated onto the cross-linked Transpin layer, and thermal imprinting was carried out at 200 °C for 1 h as before. Similar to our strategy employing a substrate modified with a PS brush, the Transpin layer attracted a majority PS block during imprint and allowed release from the PDMS-treated mold as opposed to the substrate. After release, the imprinted film was subjected to a brief CF_4 etching to remove the surface PDMS layer. In a second processing step, an O_2 plasma was used to oxidize the cylindrical domains and, simultaneously, remove the PS matrix and Transpin layer. Particular care was taken to etch only until the substrate surface was exposed to minimize undercut of the cylinders. The etched profile is shown in Figure 6a. Finally, cylindrical patterns were transferred into the underlying ~50 nm SiO_2 layer using a CHF_3 plasma etch (Figure 6b, top-down view of patterned SiO_2). The width of SiO_2 lines was ~8 nm with a pattern depth of ~10 nm, yielding an overall aspect ratio of ~1.2.

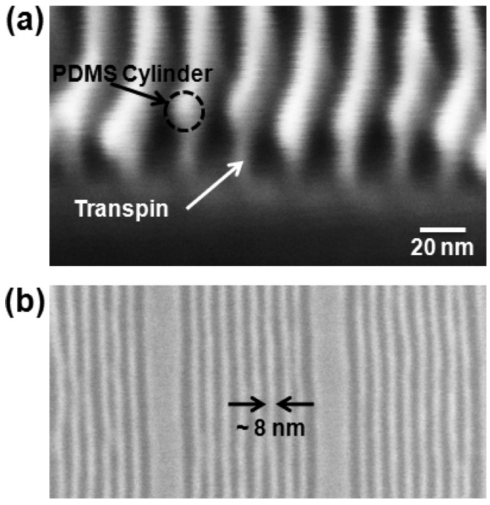

Figure 6. Sub-10 nm pattern transfer from self-assembled PS-*b*-PDMS with cylindrical patterns. (a) Tilted SEM image of block copolymer templates. (b) SiO_2 line patterns with ~8 nm width.

CONCLUSION

The combination of self-assembled polymeric resist materials and nanoimprint technique provides an easy, simple, and cost-effective way to generate ultrahigh dense arrays of ordered, sub-10 nm nanopatterns. About 0.5 μm width of mold patterns effectively guides the order of cylindrical PDMS phases in PS-*b*-PDMS thin films during thermal imprint process that finally generate linear arrays of sub-10 nm half-pitch features on the substrates. Hence, using molds that can be generated using relatively low-cost optical lithography, a 25:1 density multiplication can be achieved. Grafting PDMS brushes onto the surface of imprint mold provided for good mold-release. Notably, PDMS was not

the lowest interfacial energy treatment, yet it conferred the best results likely due to effects such as lower friction during release. In addition, we demonstrated that molds consisting of protrusive patterns over a small area of the mold improved the degree of order of block copolymer domains by preventing the interference of disordered domains from neighboring residual layers. By varying mold thicknesses and pattern geometries, we showed that flow can play a critical role in the degree of order and the speed at which order can be achieved. After obtaining a single layer of ordered block copolymer microdomains, patterns were successfully transferred to underlying SiO_2 using plasma etching. As a result, aligned single-digit nanometer features were fabricated into an underlying silicon oxide layer. These results show direct patterning of BCP using nanoimprint offers a low-cost route toward high-resolution, single-digit nanopatterning for application in plasmonics, optoelectronics, and next-generation nanoelectronics.

MATERIALS AND METHODS

Materials. BCP, polystyrene-*block*-polydimethylsiloxane (PS-*b*-PDMS−OH, $M_{n,PS}$ = 11 kg mol^{-1} and $M_{n,PDMS}$ = 5 kg mol^{-1}) with cylinder segregating morphology was purchased from Polymer Source, Inc. The silanol chain end was capped by trimethylsilyl chloride in the presence of triethylamine prior to use.[27] Microdomain spacing was measured by fast Fourier analysis as $L_0 \sim$ 20 nm with a PDMS cylinder size of ∼8 nm. Measurements were taken from SEM micrographs of BCP films vacuum annealed on a PS brush for 20 h on a PS brush followed by reactive ion etching (RIE, see below) to reveal the PDMS cylinders within the PS matrix. Polymer brushes, hydroxyl-terminated polystyrene (PS−OH, M_n = 3.7 kg mol^{-1}) and polydimethylsiloxane (PDMS−OH, M_n = 5 kg mol^{-1}), were purchased from Polymer Source, Inc. and used without further modification. Fluoroalkyl mold passivant, 1*H*,1*H*,2*H*,2*H*-perfluorodecyltrichlorosilane, was purchased from Alfa Aesar. For transfer of single-digit nanometer patterns into silicon substrates, PS-*b*-PDMS was cast onto a 13 nm Transpin (Molecular Imprints, Inc.) sacrificial layer, which was spin-coated onto the substrate from propylene glycol monomethyl ether acetate (PGMEA) and annealed in a vacuum oven at 180 °C for 10 min.

Imprint Mold Fabrication. Electron-beam lithography (EBL) was used to generate submicrometer size patterns on the photoresist films. The patterned features on the mold consisted of three linear grating where each grating was 500 μm long and extended over a width of 200 μm (200 lines). Line to space percentages were 40, 50, and 60%. The overall patterned areas on the mold had an area of 1.5×10^{-3} cm^2. To fabricate features protruding from the bulk of the mold, a negative (EBL) resist was used (ma-N, Micro Resist Technology GmbH), while to generate features that were recessed from the bulk of the mold, a positive (EBL) resist was used (PMMA, Micro Resist Technology GmbH). Electron-beam patterns were transferred onto the silicon substrates by reactive ion etching (Oxford Instruments 80+ RIE; 100 W CHF_3 10 sccm and SF_6 5 sccm, 30 mTorr). After etching, the depth of mold patterns was approximately 30 nm. Molds created by optical interference lithography were also prepared and tested (200 nm pitch). Prior to surface treatment, patterned molds were cleaned in an O_2 plasma for 15 min to remove the remaining resist and rinsed with IPA. Molds bearing fluoroalkysilane monolayer passivation were prepared *in vacuo* from vaporized fluoroalkyltrichlorosilane precursors (90 °C, $\sim 2 \times 10^{-3}$ mTorr). Monolayer thicknesses of ∼2 nm were measured by ellipsometry (Horiba Uvisel). For polymer-passivated molds, solutions of hydroxyl-terminated homopolymers of PS or PDMS were spin-coated from solutions in toluene (1% *w/w*) and thermally annealed at 170 °C for 20 h to chemically bind the end group to the substrate surface. Unbound polymer was rinsed away with toluene and IPA to leave polymer brushes with a thickness of ∼3−4 nm as determined by ellipsometry. These molds were used directly in thermal nanoimprint of PS-*b*-PDMS thin films.

Mold Cleaning between Imprints. After each use, templates were sonicated in toluene for at least 3 min and then dried under a stream of N_2.

DSA of BCP Thin Films Using Nanoimprint. Thin films of PS-*b*-PDMS were obtained by spin-coating solutions from toluene onto silicon substrates modified with a ∼3−4 nm polystyrene brush, which causes the selective segregation of the PS matrix phase to the polymer−substrate interface. Thicknesses of ∼24 nm were cast from a 0.9% w/w solution. Thermal nanoimprint with the molds bearing one of the three distinct surface passivations was subsequently performed at a pressure of ∼50 psi (0.34 MPa) using our custom-built nanoimprint tool. The imprint mold and BCP-coated substrate were sandwiched within rubber compliance layers, and the whole stack was pressed together using a pair of parallel metal plates.

Pressurized samples were annealed at 200 °C for 1 h between 50 and 200 psi to generate well-ordered BCP thin films. After cooling to room temperature (∼1 h, owing to the cooling rates of the apparatus), the pressure was released and the thin film was carefully unmolded.

The interplay of proper release mechanics and technique as the mold was separated was critical for achieving optimal macroscopic release. Initially following conventional protocols, we used a razor blade to shim and separate the components of the imprint apparatus. We found that imprint-to-imprint reproducibility was poor, owing to the sensitivity of the release mechanism to unintended and undesirable shear forces.[44] In order to overcome this problem, we implemented a more controlled release whereby the mold, fixed to one of the plates of the press, was separated from the substrate in a direction normal to the plane of the substrate (and plates). Substantial improvement was observed, although nanoscale roughness could still be observed in some of the patterned regions.

Reactive Ion Etching To Reveal BCP Microdomain Alignment. To reveal the PDMS cylinders aligned in the PS matrix, the imprinted PS-*b*-PDMS films were subjected to a sequential plasma etch (Oxford Instrument, Plasmalab 80 Plus) of CF_4 (5 s) and O_2 (10 s) to remove the PDMS surface layer and the PS matrix, respectively. The patterned images were observed using a Zeiss Ultra 60 scanning electron microscope (SEM).

Measurements of Line Edge Roughness and Line Width Roughness. Abeam Technologies myCD software was used to automatically analyze SEM images, extract contours, and find information regarding critical dimensions. The analysis is based on an understanding of physical principles involved in the formation of the SEM signal. Measurements are the average of 5 lines 450 nm long.

Pattern Transfer of Sub-10 nm Ordered BCP Domains into Silicon Substrates. Aligned cylindrical patterns in PS-*b*-PDMS films on a Transpin layer were transferred into an underlying silicon dioxide layer using a two-step dry etch: (1) 50 W CF_4 (5 s) and 90 W O_2 (35 s) to etch PS and Transpin layers; and (2) 100 W CHF_3 (15 s) to etch into the substrate anisotropically. The molds used to demonstrate pattern transfer were made for applications in electronics that required specific dimensions and ultrasmooth template sidewalls. The fabrication process is described briefly as follows: A thin layer of SiO_2 (∼50 nm) was grown on a (110)-oriented silicon-on-insulator (SOI, Silicon Quest International, Inc.) wafer by thermal oxidation. The grating patterns with 200 nm pitch were generated on the UV-curable layer (Nanonex NXR-3020) using a nanoimprinter, and imprinted structures were transferred onto the underlying SiO_2 layer using CF_4-based RIE. After removing remaining NXR-3020 layer using O_2 plasma, the

silicon layer was carefully etched to achieve 36 nm width and 24 nm height by alternation of 2% hydrofluoric acid (HF) and potassium hydroxide (KOH) etching. The (110) silicon etchant was a mixture of KOH (125 g, 3.2 mol), deionized water (400 mL), and isopropyl alcohol (100 mL), and mold etching was carried out at 65 °C. The patterned molds were treated with PDMS brush polymer before thermal imprint.

Acknowledgment. This work was supported by the Director, Office of Science, Office of Basic Energy Sciences, Materials Sciences and Engineering Division, of the U.S. Department of Energy under Contract No. DE-AC02-05CH11231. N.H. was supported by the Japan Society for the Promotion of Science (JSPS) Research Fellowships for Young Scientists and the Grant-in-Aid for JSPS Fellows (No. 22-1624).

REFERENCES AND NOTES

1. Black, C. T.; Ruiz, R.; Bretya, G.; Cheng, J. Y.; Colburn, M. E.; Guarini, K. W.; Kim, H. C.; Zhang, Y. Polymer Self Assembly in Semiconductor Electronics. *IBM J. Res. Dev.* **2007**, *51*, 605–633.
2. Kim, H. C.; Park, S. M.; Hinsberg, W. D. Block Copolymer Based Nanostructures: Materials, Processes, and Applications to Electronics. *Chem. Rev.* **2010**, *110*, 147–177.
3. Segalman, R. A. Patterning with Block Copolymer Thin Films. *Mater. Sci. Eng., R* **2005**, *48*, 191–226.
4. Stoykovich, M. P.; Nealey, P. F. Block Copolymers and Conventional Lithography. *Mater. Today* **2006**, *9*, 20–29.
5. Yang, J. K. W.; Jung, Y. S.; Chang, J.-B.; Mickiewicz, R. A.; Alexander Katz, A.; Ross, C. A.; Berggren, K. K. Complex Self-Assembled Patterns Using Sparse Commensurate Templates with Locally Varying Motifs. *Nat. Nanotechnol.* **2010**, *5*, 256–260.
6. Black, C. T. Self-Aligned Self Assembly of Multi-nanowire Silicon Field Effect Transistors. *Appl. Phys. Lett.* **2005**, *87*, 163116–163118.
7. Black, C. T.; Guarini, K. W.; Milkove, K. R.; Baker, S. M.; Russell, T. P.; Tuominen, M. T. Integration of Self-Assembled Diblock Copolymers for Semiconductor Capacitor Fabrication. *Appl. Phys. Lett.* **2001**, *79*, 409–411.
8. Park, S. M.; Stoykovich, M. P.; Ruiz, R.; Zhang, Y.; Black, C. T.; Nealey, P. E. Directed Assembly of Lamellae-Forming Block Copolymers by Using Chemically and Topographically Patterned Substrates. *Adv. Mater.* **2007**, *19*, 607–611.
9. Stoykovich, M. P.; Muller, M.; Kim, S. O.; Solak, H. H.; Edwards, E. W.; de Pablo, J. J.; Nealey, P. F. Directed Assembly of Block Copolymer Blends into Nonregular Device-Oriented Structures. *Science* **2005**, *308*, 1442–1446.
10. Park, S.; Lee, D. H.; Xu, J.; Kim, B.; Hong, S. W.; Jeong, U.; Xu, T.; Russell, T. P. Macroscopic 10-Terabit-Per-Square-Inch Arrays from Block Copolymers with Lateral Order. *Science* **2009**, *323*, 1030–1033.
11. Park, S.-M.; Craig, G. S. W.; La, Y.-H.; Solak, H. H.; Nealey, P. F. Square Arrays of Vertical Cylinders of PS-*b*-PMMA on Chemically Nanopatterned Surfaces. *Macromolecules* **2007**, *40*, 5084–5094.
12. Park, O. H.; Cheng, J. Y.; Hart, M. W.; Topuria, T.; Rice, P. M.; Krupp, L. E.; Miller, R. D.; Ito, H.; Kim, H. C. High-Aspect-Ratio Cylindrical Nanopore Arrays and Their Use for Templating Titania Nanoposts. *Adv. Mater.* **2008**, *20*, 738–742.
13. Ruiz, R.; Kang, H.; Detcheverry, F. o. A.; Dobisz, E.; Kercher, D. S.; Albrecht, T. R.; de Pablo, J. J.; Nealey, P. F. Density Multiplication and Improved Lithography by Directed Block Copolymer Assembly. *Science* **2008**, *321*, 936–939.
14. Herr, D. J. C. Directed Block Copolymer Self-Assembly for Nanoelectronics Fabrication. *J. Mater. Res.* **2011**, *26*, 122–139.
15. Cheng, J. Y.; Ross, C. A.; Smith, H. I.; Thomas, E. L. Templated Self-Assembly of Block Copolymers: Top-Down Helps Bottom-Up. *Adv. Mater.* **2006**, *18*, 2505–2521.
16. Segalman, R. A.; Yokoyama, H.; Kramer, E. J. Graphoepitaxy of Spherical Domain Block Copolymer Films. *Adv. Mater.* **2001**, *13*, 1152–1155.
17. Sundrani, D.; Darling, S. B.; Sibener, S. J. Guiding Polymers to Perfection: Macroscopic Alignment of Nanoscale Domains. *Nano Lett.* **2004**, *4*, 273–276.
18. Rockford, L.; Liu, Y.; Mansky, P.; Russell, T. P.; Yoon, M.; Mochrie, S. G. J. Polymers on Nanoperiodic, Heterogeneous Surfaces. *Phys. Rev. Lett.* **1999**, *82*, 2602–2605.
19. Cheng, J. Y.; Sanders, D. P.; Truong, H. D.; Harrer, S.; Friz, A.; Holmes, S.; Colburn, M.; Hinsberg, W. D. Simple and Versatile Methods To Integrate Directed Self-Assembly with Optical Lithography Using a Polarity-Switched Photoresist. *ACS Nano* **2010**, *4*, 4815–4823.
20. Jeong, S.-J.; Kim, J. E.; Moon, H.-S.; Kim, B. H.; Kim, S. M.; Kim, J. B.; Kim, S. O. Soft Graphoepitaxy of Block Copolymer Assembly with Disposable Photoresist Confinement. *Nano Lett.* **2009**, *9*, 2300–2305.
21. Jeong, S.-J.; Kim, S. O. Ultralarge-Area Block Copolymer Lithography *via* Soft Graphoepitaxy. *J. Mater. Chem.* **2011**, *21*, 5856–5859.
22. Jeong, S.-J.; Moon, H.-S.; Kim, B. H.; Kim, J. Y.; Yu, J.; Lee, S.; Lee, M. G.; Choi, H.; Kim, S. O. Ultralarge-Area Block Copolymer Lithography Enabled by Disposable Photoresist Prepatterning. *ACS Nano* **2010**, *4*, 5181–5186.
23. Guo, L. J. Nanoimprint Lithography: Methods and Material Requirements. *Adv. Mater.* **2007**, *19*, 495–513.
24. Schift, H. Nanoimprint Lithography: An Old Story in Modern Times? A Review. *J. Vac. Sci. Technol., B* **2008**, *26*, 458–480.
25. Jung, G.-Y.; Li, Z.; Wu, W.; Chen, Y.; Olynick, D. L.; Wang, S.-Y.; Tong, W. M.; Williams, R. S. Vapor-Phase Self-Assembled Monolayer for Improved Mold Release in Nanoimprint Lithography. *Langmuir* **2005**, *21*, 1158–1161.
26. Hu, Z.; Finlay, J. A.; Chen, L.; Betts, D. E.; Hillmyer, M. A.; Callow, M. E.; Callow, J. A.; DeSimone, J. M. Photochemically Cross-Linked Perfluoropolyether-Based Elastomers: Synthesis, Physical Characterization, and Biofouling Evaluation. *Macromolecules* **2009**, *42*, 6999–7007.
27. Voet, V. S. D.; Pick, T. E.; Park, S.-M.; Moritz, M.; Hammack, A. T.; Urban, J. J.; Ogletree, D. F.; Olynick, D. L.; Helms, B. A. Interface Segregating Fluoralkyl-Modified Polymers for High-Fidelity Block Copolymer Nanoimprint Lithography. *J. Am. Chem. Soc.* **2011**, *133*, 2812–2815.
28. Li, H.-W.; Huck, W. T. S. Ordered Block-Copolymer Assembly Using Nanoimprint Lithography. *Nano Lett.* **2004**, *4*, 1633–1636.
29. Man, X.; Andelman, D.; Orland, H.; Thebault, P.; Liu, P. H.; Guenoun, P.; Daillant, J.; Landis, S. Organization of Block Copolymers Using Nanoimprint Lithography: Comparison of Theory and Experiments. *Macromolecules* **2011**, *44*, 2206–2211.
30. Kim, S.; Lee, J.; Jeon, S.-M.; Lee, H. H.; Char, K.; Sohn, B.-H. Orientation of Lamellar Nanostructures in the Patterned Thin Films of a Diblock Copolymer. *Macromolecules* **2008**, *41*, 3401–3404.
31. Politakos, N.; Ntoukas, E.; Avgeropoulos, A.; Krikorian, V.; Pate, B. D.; Thomas, E. L.; Hill, R. M. Strongly Segregated Cubic Microdomain Morphology Consistent with the Double Gyroid Phase in High Molecular Weight Diblock Copolymers of Polystyrene and Poly(Dimethylsiloxane). *J. Polym. Sci., Part B: Polym. Phys.* **2009**, *47*, 2419–2427.
32. Jung, Y. S.; Chang, J. B.; Verploegen, E.; Berggren, K. K.; Ross, C. A. A Path to Ultranarrow Patterns Using Self-Assembled Lithography. *Nano Lett.* **2010**, *10*, 1000–1005.
33. Takenaka, M.; Aburaya, S.; Akasaka, S.; Hasegawa, H.; Hadjichristidis, N.; Sakellariou, G.; Tada, Y.; Yoshida, H. Formation of Long-Range Stripe Patterns with Sub-10-nm Half-Pitch from Directed Self-Assembly of Block Copolymer. *J. Polym. Sci., Part B: Polym. Phys.* **2010**, *48*, 2297–2301.
34. Xiao, S.; Yang, X.; Lee, K. Y.; ver der Veerdonk, R. J. M.; Kuo, D.; Russell, T. P. Aligned Nanowires and Nanodots by Directed Block Copolymer Assembly. *Nanotechnology* **2011**, *22*, 305302.
35. Odom, T. W.; Love, J. C.; Wolfe, D. B.; Paul, K. E.; Whitesides, G. M. Improved Pattern Transfer in Soft Lithography Using Composite Stamps. *Langmuir* **2002**, *18*, 5314–5320.

36. McNaught, A. D.; Wilkinson, A. *IUPAC, Compendium of Chemical Terminology*, 2nd ed.; Blackwell Scientific Publications: Oxford, 1997.
37. Lee, M. J.; Lee, N. Y.; Lim, J. R.; Kim, J. B.; Kim, M.; Baik, H. K.; Kim, S. K. Anti-adhesion Surface Treatments of Molds for High Resolution Unconventional Lithography and Applications. *Adv. Mater.* **2006**, *18*, 3115–3119.
38. Thanawala, S. K.; Chaudhury, M. K. Surface Modification of Silicone Elastomer Using Perfluorinated Ether. *Langmuir* **2000**, *16*, 1256–1260.
39. Newby, B.-M. Z.; Chaudhury, M. K.; Brown, H. R. Macroscopic Evidence of the Effect of Interfacial Slippage on Adhesion. *Science* **1995**, *269*, 1407–1409.
40. Kannan, R. M.; Kornfield, J. A. Evolution of Microstructure and Viscoelasticity during Flow Alignment of a Lamellar Diblock Copolymer. *Macromolecules* **1994**, *27*, 1177–1186.
41. Scheer, H. C.; Bogdanski, N.; Wissen, M.; Konishi, T.; Hirai, Y. Polymer Time Constants during Low Temperature Nanoimprint Lithography. *J. Vac. Sci. Technol., B* **2005**, *23*, 2963–2966.
42. Sundrani, D.; Darling, S. B.; Sibener, S. J. Hierarchical Assembly and Compliance of Aligned Nanoscale Polymer Cylinders in Confinement. *Langmuir* **2004**, *20*, 5091–5099.
43. Labrake, D., Director of Applications, Molecular Imprints, Inc., Austin, TX, 2011, personal communication.
44. Landis, S.; Chaix, N.; Gourgon, C.; Leveder, T. Quantitative Characterizations of a Nanopatterned Bonded Wafer: Force Determination for Nanoimprint Lithography Stamp Removal. *Nanotechology* **2008**, *19*, 125305–125417.
45. Wu, S. *Polymer Interface and Adhesion*; Marcel Dekker: New York, 1982; p 615.
46. Morita, M.; Koga, T.; Otsuka, H.; Takahara, A. Macroscopic-Wetting Anisotropy on the Line-Patterned Surface of Fluoroalkylsilane Monolayers. *Langmuir* **2004**, *21*, 911–918.